applied optics

Hands-On Photonic Education Kits: empowering the integrated photonics workforce through practical training

Lilian Neim,[1] Alexander Yovanovich,[1] Jacob Bartholomew,[1] Venkatesh Deenadayalan,[1] Mario Ciminelli,[1] Thomas Palone,[1] Matthew van Niekerk,[1] Meiting Song,[2] Arunima Nauriyal,[2] Jelena Notaros,[3] Samuel Serna Otálvaro,[4] Jaime Cardenas,[2] Thomas Brown,[2] Anuradha Murthy Agarwal,[5] Sajan Saini,[5] and Stefan F. Preble[1,*]

[1]Microsystems Engineering, Rochester Institute of Technology, Rochester, New York 14623, USA
[2]The Institute of Optics, University of Rochester, Rochester, New York 14627, USA
[3]Research Laboratory of Electronics, Massachusetts Institute of Technology, Cambridge, Massachusetts 02139, USA
[4]Bridgewater State University, Bridgewater, Massachusetts 02324, USA
[5]Department of Materials Science and Engineering, Massachusetts Institute of Technology, Cambridge, Massachusetts 02139, USA
*sfpeen@rit.edu

Received 3 August 2023; revised 27 September 2023; accepted 29 September 2023; posted 2 October 2023; published 17 October 2023

The Hands-On Photonic Education (HOPE) Kits, developed with AIM Photonics, address the need for skilled workers in integrated photonics. This paper highlights the role of the HOPE Kits in advancing the training ecosystem and bridging the skills gap. The kits include fully packaged photonic integrated circuits (PICs), enabling instructors to educate and train students on PIC testing and characterization. Covering a wide range of devices and circuits, from waveguides to wavelength division multiplexing for data communication, the kits offer a hands-on experience. Engaging with actual PICs, students gain practical insights, enhancing their understanding of key principles, and preparing them for real-world skill sets in integrated photonics.

https://doi.org/10.1364/AO.502232

1. INTRODUCTION

In advanced manufacturing industries such as optics and photonics, there is a critical need for trained and skilled workers. The characteristics of photonics and optics technologies necessitate specialized knowledge and expertise [1,2]. However, existing training programs often struggle to keep pace with the rapidly evolving field. There is a pressing need for training initiatives that demonstrate a deep understanding of the current technology landscape and anticipate future advancements [3,4]. This is particularly the case for integrated (silicon-based) photonics, which is a key technology for data communication (datacom) applications [5,6], and is emerging as a promising technology for applications in sensing [7], quantum [8], artificial intelligence [9], LiDAR [10], and more. The integrated photonics education community is working to address the challenge of training in this rapidly evolving field and is playing a critical role in improving the integrated photonics training ecosystem with the development of courses (in-person and online), workshops, simulation tools, and PIC chips focused on educational concepts [11–15]. In response to the need, the Hands-On Photonic Education (HOPE) Kits described in this paper are being developed with the support of the American Institute for Manufacturing Photonics (AIM Photonics) [16]. These kits offer instructors a practical and accessible solution for educating and training students on photonic integrated circuit (PIC) testing and characterization.

The HOPE Kits consist of fully packaged PICs (Fig. 1), eliminating the complexities and costs associated with bare-PIC alignment setups. They have been designed to start from basic PIC concepts, such as insertion loss and interference, and gradually build up to cover key datacom devices and circuits, including modulators, photodetectors, filters, and wavelength division multiplexing. By providing students with the opportunity to test and study actual PICs, the HOPE Kits enhance their understanding of fundamental PIC principles and prepare them for the challenges of real-world applications (in particular, datacom—which is the primary application of PICs today). This paper focuses on the significance of the HOPE Kits in addressing the skills gap in the photonics workforce. By enabling hands-on experience and practical learning, these kits contribute to improving the photonics training ecosystem. The

Fig. 1. Datacom HOPE kit with six packaged PICs (Chip 1: insertion loss; Chip 2: interference; Chip 3: Mach–Zehnder modulation; Chip 4: germanium photodetectors; Chip 5: ring resonators and wavelength division multiplexing; Chip 6: ring resonator modulation) covering the fundamental concepts of data communication.

paper emphasizes the need for innovative approaches to training and highlights the role of the integrated photonics community in driving these advancements. Ultimately, the HOPE Kits offer a valuable tool for empowering the photonics workforce and ensuring the continued growth and success of the integrated photonics industries.

2. OVERVIEW OF THE HOPE KITS-SIX CHIPS

The Datacom HOPE Kit comprises six PICs, as shown in Fig. 1 (HOPE Kit with six packaged PICs) and Fig. 2 (microscope image of each PIC), that cover a wide range of topics and functionalities [5,6]. Each PIC offers unique learning opportunities and contributes to the comprehensive understanding of integrated photonic concepts, as follows.

1. HOPE Chip 1: Insertion Loss
   Focuses on the characterization of insertion loss in PICs. It covers important parameters such as waveguide propagation loss, bend loss, and fiber-to-chip coupling loss [5,6]. By studying this chip, students gain insights into the factors influencing signal loss and learn techniques for minimizing losses in practical photonic systems.
2. HOPE Chip 2: Interference
   Explores the principles of interference in photonics [5,6]. It utilizes directional couplers, y-branch devices, and Mach–Zehnder interferometers to demonstrate interference phenomena. Additionally, students learn how to control interference using thermo-optic phase shifting. This chip deepens their understanding of interference effects and their practical applications.
3. HOPE Chip 3: Mach–Zehnder Modulation
   Delves into the realm of Mach–Zehnder modulation [17,18]. Students explore thermo-optically and electro-optically phase-shifted Mach–Zehnder interferometers, utilizing PIN and PN reverse biasing configurations. This chip provides hands-on experience in manipulating the modulation characteristics of photonic devices, enabling students to understand the operation and performance of modulators.
4. HOPE Chip 4: Germanium Photodetectors
   Focuses on the characterization of germanium photodetectors [5,19,20]. Students learn about crucial parameters such as dark current, responsivity, and quantum efficiency. This chip also includes a complete Mach–Zehnder modulator link, showcasing a complete transceiver on a single PIC. Students gain practical knowledge of photodiode characterization and its applications in optical communication systems.
5. HOPE Chip 5: Wavelength Division Multiplexing
   Introduces students to wavelength division multiplexing (WDM) using ring resonators [5,6,21]. It covers different types of ring resonators, including single-bus and double-bus configurations. Students gain insights into important characteristics such as over/critical/under coupling, quality factor, free spectral range, and extinction ratio. Moreover, this chip offers hands-on experience in WDM multiplexing and demultiplexing techniques using ring-resonator-based structures.
6. HOPE Chip 6: WDM Ring Modulators
   Focuses on WDM ring modulators, specifically micro-ring modulators utilizing a PIN junction [22]. Students explore the operation of microring modulators, including the tradeoffs in efficiency, bandwidth, and loss. Additionally, this chip covers the implementation of a WDM microring modulation transmitter, providing a practical understanding of WDM modulation techniques.

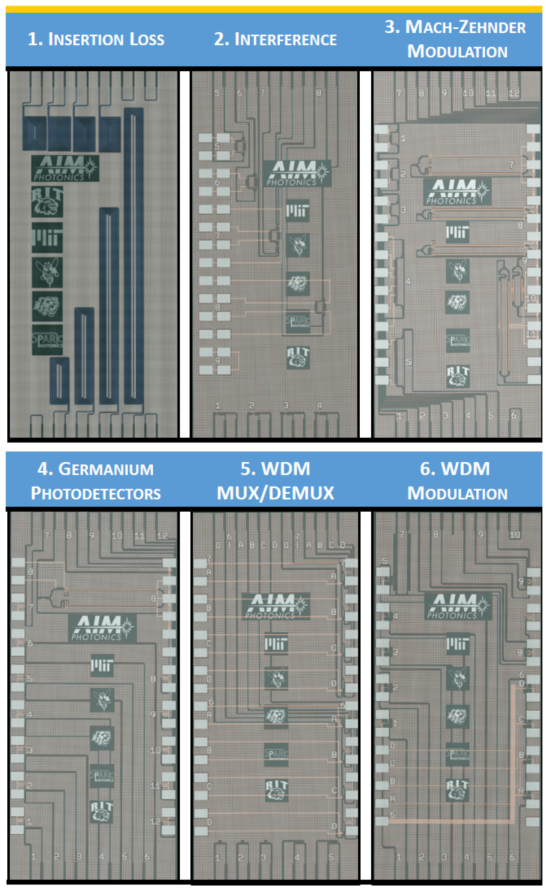

Fig. 2. Microscope images of the six Datacom HOPE Kit PIC chips.

The Datacom HOPE Kit offers the flexibility to study and characterize each PIC individually. However, students can also combine multiple PICs to create a complete wavelength division multiplexing data communication system. This integration allows for a holistic learning experience, enabling students to apply their knowledge across different PICs and gain practical insights into the implementation of advanced photonic technologies.

3. PACKAGING, TESTING, AND STANDARD SETUP

The HOPE Kits are designed with a standardized package configuration, ensuring consistency and ease of use across all the PICs included in the kit. This section provides an overview of the packaging, testing, and standard setup employed for the HOPE Kits.

A. PIC Package Configuration

All PICs in the kit utilize an identical package, as depicted in Fig. 1. Each package has a printed circuit board (PCB) mounted on a base plate.

B. Fiber Arrays and Polarization

To facilitate optical connectivity, there are 12-channel polarization-maintaining (PM) fiber arrays connected on one side with fiber arrays 1–12 and on the other side with fiber arrays 13–24 of each PIC, as seen in Fig. 3. The optical fibers are equipped with FC/UPC connectors, with the slow axis of the fiber aligned with the connector key. It is essential to ensure that the laser's polarization aligns with the key. If misaligned, an adapter such as a connector or a PM optical fiber that rotates the polarization axis can be utilized. Alternatively, a polarization controller can be employed. Most of the devices on the PICs are designed to operate with transverse electric (TE) polarization. The fiber arrays attached to the PIC are oriented so that the polarization launched into the PIC is horizontally (TE) polarized.

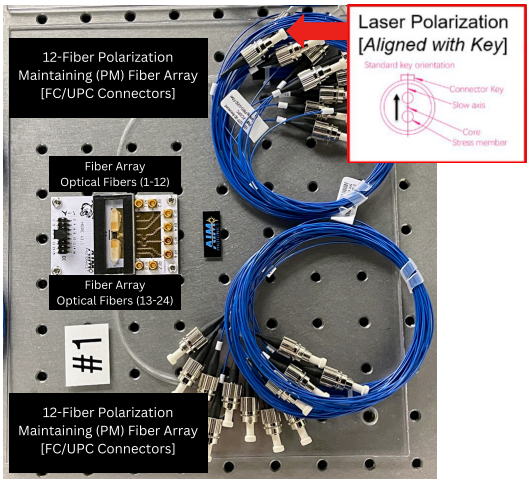

Fig. 3. HOPE package consisting of a PCB on base plate with two 12-fiber polarization-maintaining fiber arrays connected to each PIC.

C. Electrical Connections

Each PCB has DC (low frequency) and RF (high frequency) electrical connections, shown in Fig. 4. The PCB features 16 DC header pin connections on the left side, arranged in a two-row, eight-column grid. These can be connected using a standard spaced GPIO (general-purpose input/output) ribbon cable with a 2×8 female connector. Alternatively, individual female jumper wires can be used. The RF connections are designed for a 50 ohm impedance and utilize SMP connectors (male). SMP (female) cables are required for the connections. It is recommended to use short microwave adapter cables from SMP (female) to SMA (female) and leave them connected to the PCB to minimize the number of connects/disconnects to preserve longevity.

D. Standard Testing Configuration

Figure 5 illustrates a typical testing configuration utilized for a single HOPE PIC. The optical equipment required includes a tunable laser and at least one photodetector. An optional polarization controller is also shown. The students will need to change the optical fiber and electrical connections to test the various circuits in the PICs. If a lab has suitable switching equipment, it should be used to simplify the connectivity to all of the circuits. For electrical measurements, a source meter, oscilloscope, and waveform generator are primarily needed. The packaging, testing, and standard setup described above provide a solid foundation for utilizing the HOPE Kits and conducting experiments with the included PICs. By adhering to the recommended procedures and precautions, users can ensure proper functionality, accurate measurements, and longevity of the components. Alternatively, these procedures can be adapted to testing bare PIC chips using a suitable photonic/electronic test setup consisting of alignment stages and electrical probes. Bare PIC testing provides students with additional experience in optical alignment and electrical probing.

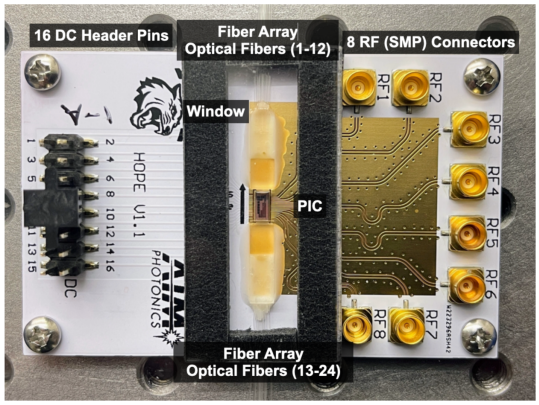

Fig. 4. HOPE PCB with PIC mounted in the middle, fiber arrays 1–24, 16 DC header pins (for applying/reading electrical signals at low frequencies), and eight RF (SMP) connectors for high-speed signals applied/read to the PIC.

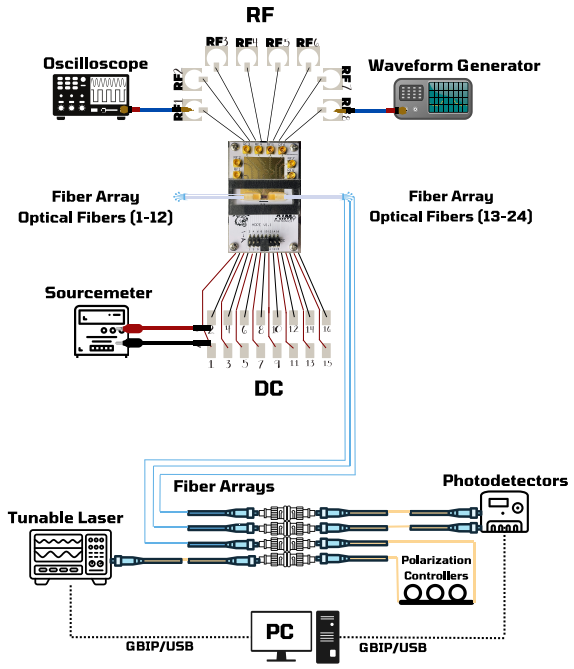

Fig. 5. Typical PIC setup and connectivity.

4. EXAMPLE EXPERIMENTAL DEMONSTRATION WITH HOPE KITS-WAVELENGTH DIVISION MULTIPLEXING USING MICRORINGS

As an example to highlight how the HOPE Kit can be used for training, this section of the paper presents an experimental demonstration focused on the implementation of wavelength division multiplexing (WDM) and modulation using microring devices and circuits. WDM is a widely used technology in optical communication systems [6]. It allows multiple optical signals to be transmitted over a fiber optic cable by separating them into different wavelength channels, each carrying a different data stream. The multiplexer combines the signals, and the demultiplexer separates them at the receiver end, directing them to the appropriate receiver [23,24]. WDM technology increases data transmission capacity and efficiency, making it an essential component of modern high-speed internet and communication networks. There are a variety of techniques for realizing WDM on a PIC [6,25], including the use of interferometers [26], arrayed waveguide gratings (AWGs) [25], Bragg filters [27], and microring resonators [21]. In the HOPE kit we utilize microrings due to their compact size, flexibility, and tunability. Specifically, a ring resonator is a closed-loop waveguide ("ring waveguide") placed in close proximity to a bus waveguide. Light is able to tunnel to/from the bus into the ring resonator. Resonance occurs when there is an integer multiple of light waves within the circumference of the ring, which is expressed as [5]

$$2\pi R = \frac{\lambda_{\text{res}} m}{n_{\text{eff}}}, \tag{1}$$

where "m" is an integer, n_{eff} is the effective index of the ring waveguide, and λ_{res} is a resonant wavelength (corresponding to a specific "m"). There are several key parameters that are typically tested [5].

The quality factor (Q) quantifies the sharpness of resonance, and it is defined as

$$Q = \frac{\lambda_{\text{res}}}{\Delta\lambda}, \tag{2}$$

such that $\Delta\lambda$ is the full width at half maximum (FWHM) of the resonance in the transmission spectrum. The free spectral range (FSR) represents the spacing between consecutive resonant wavelengths in a ring resonator and is calculated as

$$\text{FSR} = \frac{\lambda^2}{n_g L} = \frac{\lambda^2}{n_g 2\pi R}, \tag{3}$$

where n_g is the group index of the ring waveguide. The extinction ratio (ER) measures the difference in power between the transmitted light when the ring resonator is on-resonance and when it is off-resonance. It is often expressed in decibels (dB) and calculated as

$$\text{ER}(dB) = \text{abs}\left(10\log 10\left(\frac{P_{\text{on}}}{P_{\text{off}}}\right)\right), \tag{4}$$

where P_{on} is the transmitted power on-resonance, and P_{off} is the transmitted power off-resonance.

Figure 6 illustrates how multiple ring resonators with different radii in series are utilized to realize a WDM system [28]. Specifically, with add–drop ring resonators, specific wavelengths can be added (multiplex: MUX) or dropped (demultiplex: DEMUX), by sending signals through the resonator's appropriate add–drop ports. In order to ensure that each resonator can be tuned to a particular wavelength of interest, each ring incorporates an integrated thermal heater implemented using a DC tuned resistor placed in close proximity to the ring resonator, as illustrated in Fig. 6. This design enables precise fine-tuning by leveraging the thermo-optic effect. This effect describes how the refractive index of a material changes with temperature. When voltage is applied to the resistor placed near the ring resonator, it generates heat. This localized heating raises the temperature in the proximity of the ring. As a result, the refractive index of the waveguide material in that area changes and effectively shifts the resonant wavelengths of the microring resonator. The temperature-dependent wavelength shift can be expressed by

$$\frac{d\lambda}{dT} = \frac{\lambda}{n_g}\left(\frac{dn_{\text{eff}}}{dT}\right), \tag{5}$$

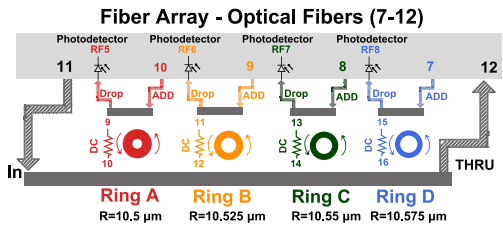

Fig. 6. Illustration of HOPE-Kit Chip-5 device, displaying four ring resonators with different radii utilized for a single WDM setup. The false colors represent four different wavelengths of operation. Additionally, the diagram showcases the various optical, RF, and DC connections summarized in Fig. 5.

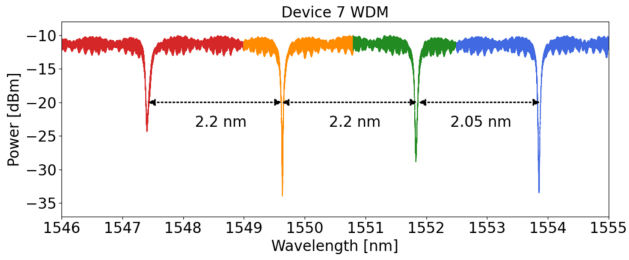

Fig. 7. False-colored (corresponding to Rings A, B, C, and D in Fig. 6) transmission spectrum showcasing the resonance spacing.

where n_{eff} is the effective index, n_g is the group index, and (dn_{eff}/dT) is the rate change of the effective index with respect to temperature [29,30].

A. WDM MUX/DEMUX

The assessment begins with an overall identification of the microring resonances. Specifically, the students are instructed to connect a laser to the in port and a detector to the thru port. A wavelength sweep is performed within the range of 1500–1600 nm with a laser connected to obtain the transmission spectrum shown in Fig. 7, which is false-colored to indicate the resonances for the four ring resonators. The most important metric is the spacing of the resonances, which was designed to be approximately 2 nm. The ring resonances exhibit sharp filtering with extinction of signals at the resonance wavelength of $>10-20$ dB. The students are instructed to analyze the main characteristics of the resonances, namely, the quality factor (sharpness), extinction (depth), and relative spacings [including the concept of free spectral range (FSR), not shown in this short example].

The resonant spacings are a key aspect of WDM and are controlled by applying electrical power to the individual rings using specific voltages determined by the heater resistance. The students must closely monitor the heaters' effects on the channel spacing. Specifically, their objective is to fine-tune the spacing between the resonances of Rings A–D, as shown in Fig. 7. This hands-on experimentation allows them to gain practical insight into the device's responsiveness and control mechanisms. This information is crucial for assessing the performance and functionality of the WDM circuit.

Next, the students investigate how the ring resonator can be used to realize a WDM MUX where a specific wavelength signal is added. The students specifically connect the laser to the add port of Ring A, and the detector is connected to the common optical thru port (Fig. 6). The results shown in Fig. 8 are analyzed where the students observe the high transmission of wavelengths corresponding to Ring A. The students can assess the bandwidth of the transmission peak and also note any loss that is obtained relative to thru-port transmission in Fig. 7. Notable results seen in Fig. 8 are the three negative dips corresponding to Rings B, C, and D. These dips occur because Ring A continues to transmit light from the add-to-thru port but just at an attenuated level. The attenuated light subsequently undergoes further filtering by Rings B, C, and D as it propagates past those three resonators. The amount of off-resonant light

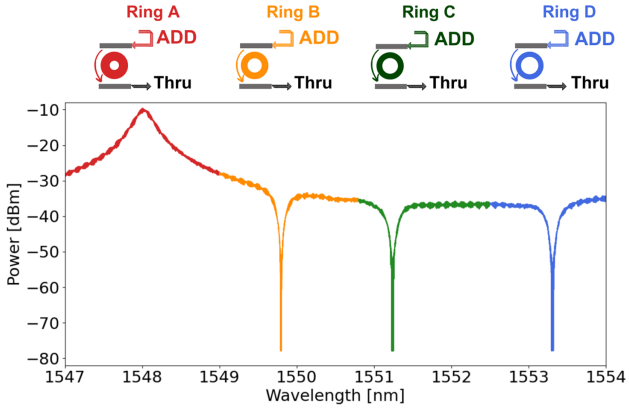

Fig. 8. False-colored transmission spectrum of Ring A's add-to-thru port. The transmission spectrum has high transmission for Ring A, while the other three resonances are visible as background drops in transmission at the respective resonances for Rings B, C, and D.

coupled across Ring A is determined by the coupling coefficients $\kappa_{\text{thru, drop}}$ between the waveguide and the resonators. The strength of the coupling determines how off-resonant wavelengths are suppressed but has a tradeoff in the bandwidth (quality factor) and loss of the resonance.

Lastly, we focus on the WDM DEMUX designed to drop a signal at a specific wavelength and detect it with a photodetector to directly generate an electrical signal. Figure 9 shows the resulting photocurrent for Ring A measured as the laser's wavelength is swept across the resonance. By measuring the photocurrent signal at the drop port, students gain valuable insights into the DEMUX's behavior and its ability to filter and ultimately detect optical signals at specific wavelengths. The students can investigate any cross-talk between photodetectors on Rings B, C, and D. Lastly, the WDM MUX/DEMUX can be combined with modulation in order to demonstrate a complete optical link. In the next section, we discuss the specifics of a microring modulator suitable for modulation in a WDM system.

B. PIN Microring Modulator

Microring modulators are realized by integrating a diode into the silicon microring resonator as shown in Fig. 10. There are different configurations but the simplest (and first demonstrated in the field) is a PIN diode consisting of three regions: P-type, intrinsic (I)-type, and N-type. The P- and N-regions

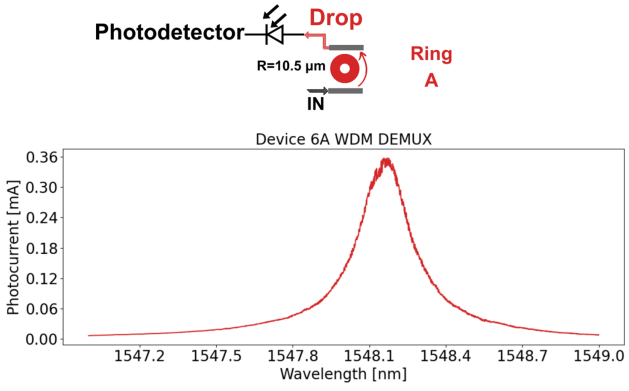

Fig. 9. Photocurrent measured at the drop port of Ring A.

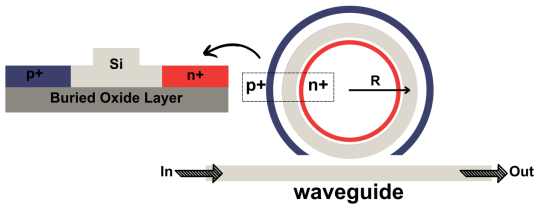

Fig. 10. PIN microring modulator illustration.

are doped with impurities to introduce free carriers (electrons or holes) into the material. The I-region (intrinsic) has very low impurity doping, resulting in fewer free carriers [31], and is the primary waveguide region used to guide the light around the ring. When a forward biased is applied (by applying a positive voltage to the P-region relative to the N-region), free carriers diffuse into the instrinsic waveguide region. The free carriers change the refractive index and absorption of the silicon by virtue of the free carrier plasma dispersion effect (FCPDE) [32,33]. The FCPDE can be quantified through the calculations of the free carrier induced index change (Δn) and free carrier absorption change ($\Delta\alpha$):

$$\Delta\alpha(\lambda) = \Delta\alpha_e(\lambda) + \Delta\alpha_h(\lambda) = a(\lambda)\Delta N_e^{b(\lambda)} + c(\lambda)\Delta N_h^{d(\lambda)}, \tag{6}$$

$$-\Delta n(\lambda) = \Delta n_e(\lambda) + \Delta n_h(\lambda) = p(\lambda)\Delta N_e^{q(\lambda)} + r(\lambda)\Delta N_h^{s(\lambda)}, \tag{7}$$

where $a = 8.8 \times 10^{-21}\text{cm}^2$, $b = 1.167$, $c = 5.84 \times 10^{-20}\text{cm}^2$, $d = 1.109$, $p = 5.40 \times 10^{-22}\text{cm}^3$, $q = 1.011$, $r = 1.53 \times 10^{-18}\text{cm}^3$, $s = 0.838$ are the coefficients of $\Delta\alpha(\lambda)$ and $-\Delta n(\lambda)$ at 1550 nm wavelength as found in [33].

The free carriers result in a significant change in the ring resonance. Specifically, the resonant wavelength shifts [calculated using Eq. (1)] due to the change in n_{eff} as a result of the free carrier refractive index change from Eq. (6). In addition, the change in absorption [Eq. (7)] also changes the extinction ratio of the ring [as measured using Eq. (4)] due to the increased loss. Consequently, by alternating the voltage applied to the PIN diode, light with a wavelength tuned near a resonance can be modulated on or off by these resonance changes.

The objective of this experiment is to investigate the performance of the PIN microring modulators and gain insights into the modulation behavior of the modulators under different bias conditions. Figure 11 illustrates the layout of the microring modulator devices featured on HOPE Kit Chip 6. There are five PIN microring modulators with the same radius while the coupling gap varies. The students are instructed to identify the optimal device and understand the tradeoffs in coupling strength (determined by the waveguide–ring coupling gap) and the resonant response of the devices.

Figure 12 shows the results of the experiment for Device 1. The transmission spectrum is measured with a DC forward-bias voltage ranging from 0 V to 1.2 V. The students first learn that the resonance wavelength of the resonator shifts towards a shorter wavelength (blue shifts) as the forward-bias voltage increases. This is because as free carriers are injected into the waveguide, the refractive index reduces. Next, the students observe that the shape, in particular the width and depth, of the

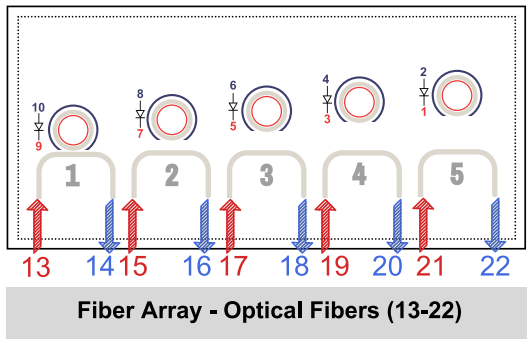

Fig. 11. Layout of PIN microring modulator devices integrated in HOPE Kit Chip 6.

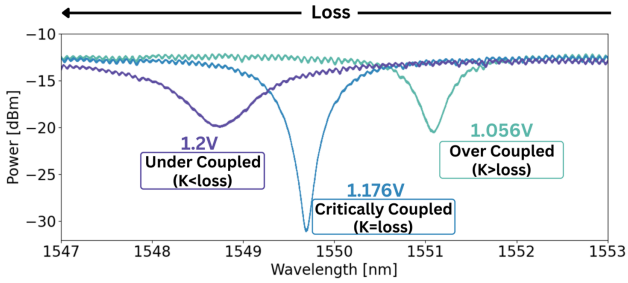

Fig. 12. HOPE Chip 6, Device 1 PIN microring modulator response as the forward-bias voltage varies. The resonator goes through three coupling regimes: over coupled, critically coupled, and under coupled.

resonance drastically changes. This is because as this forward-bias increases, the free carriers also significantly increase the loss of the waveguide due to free carrier absorption (FCA). At a low voltage (1.056 V and less), the FCA is relatively low, and the resonator is subsequently over coupled, where the coupling coefficient (κ) is greater than the ring loss ($\kappa >$ loss). As we increase the voltage (1.176 V), the resonance becomes critically coupled because the ring loss is increased to the point where it matches the coupling coefficient from the waveguide-to-ring ($\kappa =$ loss). However, when the voltage is further increased (1.2 V) the FCA loss exceeds the coupling loss, resulting in the resonator becoming under coupled ($\kappa <$ loss). This demonstration allows students to gain insight into the factors that influence the resonance condition. Specifically, by simply changing the voltage applied to the device, the students can observe the three regimes of resonant coupling. Furthermore, they learn how using a PIN diode can modulate the resonant wavelength of a microring modulator.

Finally, we demonstrate modulation using on–off-keying (OOK) with a square-wave applied to the modulator. A PIN microring device with a coupling gap that achieves critical coupling at 0 mV was selected. The bottom of Fig. 13 shows the measured wavelength response of the microring modulator when 0 mV and 930 mV are applied to the modulator. The 930 mV high voltage was selected to optimize the free carrier response of the device relative to any thermo-optic effects experienced by the device (i.e., higher voltages result in significant thermal transients). By applying a square-wave with low/high

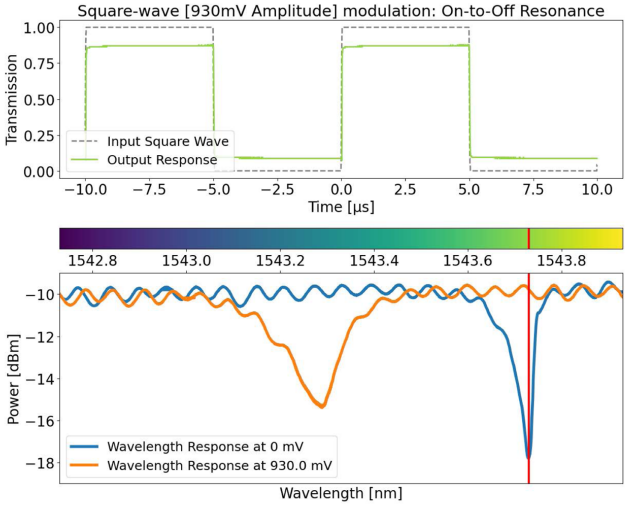

Fig. 13. PIN microring modulator response to a square-wave [930 mV amplitude] and laser tuned for on-to-off resonance modulation. The bottom plot shows the wavelength response of the resonator at 0 mV and 930 mV, and the vertical line indicates where the laser is set for modulation.

amplitudes of 0 mV and 930 mV, the resonance is shifted back-and-forth between the two resonance conditions shown at the bottom of Fig. 13. By tuning the laser (vertical line at the bottom of Fig. 13) to be on-resonance at 0 mV, we observe that the transmission follows the applied square-wave. Specifically, when the voltage is 0 mV, the transmission is low because the resonator is on-resonance. When the voltage is 930 mV, the transmission is high because the resonator is now off-resonance.

The opposite response (off-to-on resonance) is shown in Fig. 14 where the laser is tuned to be aligned to the 930 mV resonance (vertical line at the bottom of Fig. 14). In this case, when the square-wave is at 0 mV, the transmission is high because the resonator is off-resonance. And when the square-wave is at 930 mV, the transmission is now low because the resonator moves to be on-resonance. If the wavelength of the laser is in between these two extremes shown in Figs. 13,14, modulation responses will vary drastically. In particular, if the laser is tuned far away from these resonances, no modulation will be observed at all. The important takeaway for the students is that microring modulators are highly wavelength selective. Specifically, they will only modulate laser light at wavelengths specifically aligned to the resonant wavelength of the modulator. Lastly, the modulation rate used here was relatively low (200 kb/s) in order to illustrate the basic concepts of modulation at speeds typically accessible in most university electrical laboratory settings. With more advanced test equipment, the response of the modulators can be assessed at higher speeds.

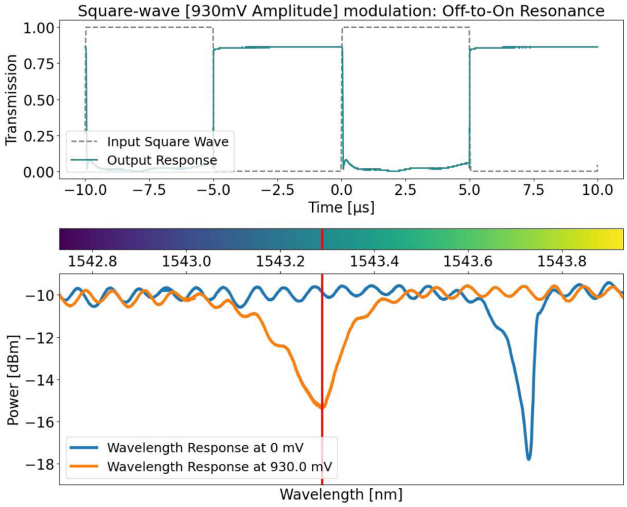

Fig. 14. PIN microring modulator response to a square-wave [930 mV amplitude] and laser tuned for off-to-on resonance modulation. The bottom plot shows the wavelength response of the resonator at 0 mV and 930 mV, and the vertical line indicates where the laser is set for modulation.

5. EDUCATIONAL METHODOLOGY: HANDS-ON PIC TESTING WORKSHOPS AND IMPLICATIONS FOR THE INTEGRATED PHOTONICS TRAINING ECOSYSTEM

Our educational approach involves hands-on PIC testing workshops [34], which are designed to enhance students' comprehension of photonics concepts and their practical application using the HOPE Kits. Those interested in utilizing the kits in their own education initiatives can find more information at the website in [34] and are also encouraged to contact Professor Preble. Here is a comprehensive overview of our methodology and its implications for the integrated photonics training ecosystems.

1. Participant Selection
   Students were chosen from a pool of individuals enrolled in a photonics-related program. Selection criteria included a foundational understanding of photonics concepts and a willingness to participate in the workshop.
2. Pre-Test Assessment
   Before the hands-on training, participants attended a comprehensive one-day presentation covering the fundamental principles of photonics relevant to the operation of the HOPE Kits. This session gave participants the necessary background knowledge to engage effectively in the subsequent training.
3. Hands-On Training Workshop
   Participants participated in a four-day workshop on hands-on training with the HOPE Kits. This immersive experience allowed participants to work extensively with the included PICs, focusing on different topics and experiments that spanned various photonics concepts and practical applications. Additionally, all participants were provided with excerpts from an instructor's guide, which offers detailed explanations of the theory behind each experiment in the HOPE Kit. This guide served as an invaluable resource, helping both instructors and students understand the kit activities and get an overview of the theory and guidance on the expected outcomes from the hands-on activities, thereby enhancing the overall learning experience.
4. Experimental Procedures and Data Analysis
   Throughout the workshop, participants followed detailed experimental procedures outlined in a comprehensive

written script. The script guided setting up, operating, and collecting data for each experiment. Participants were encouraged to analyze the gathered data using the script and respond to accompanying questions, fostering result interpretation and comprehension of underlying photonics principles.

5. Data Interpretation and Understanding
Active engagement in the hands-on training workshop allowed participants to interpret the collected data and deepen their grasp of the photonics concepts addressed in each experiment. The iterative nature of the workshop facilitated reinforcing knowledge, establishing connections between theoretical concepts and experimental outcomes, and fostering a comprehensive understanding of the covered topics.

A. Implications for the Integrated Photonics Training Ecosystem

The development and implementation of the HOPE Kits have far-reaching implications for the integrated photonics training ecosystem. As the demand for skilled workers in advanced manufacturing industries such as optics and photonics continues to rise [3], the need for effective and up-to-date training initiatives becomes paramount. The HOPE Kits present a valuable solution to address the challenges associated with traditional teaching methods and bridge the gap between theoretical knowledge and practical application.

One of the key implications of the HOPE Kits is the shift from passive learning to active engagement, as illustrated in Fig. 15. Traditional lecture-based instruction often leaves students with limited opportunities for hands-on experimentation and real-world applications [1,12]. However, the HOPE Kits provide an immersive learning experience that allows students to interact directly with PICs and gain practical insights into their functionalities. Through hands-on experimentation, students can deepen their understanding of photonics concepts and develop essential skills relevant to the integrated photonics industry. Moreover, exposure to a diverse set of devices equips students with a comprehensive skill set that extends beyond what is typically taught at the undergraduate level. As a result, graduates trained with the HOPE Kits are better prepared to enter the photonics industry as middle-skilled labor, filling the crucial gap between entry-level technicians and highly specialized engineers.

The practical approach of the HOPE Kits also addresses the challenge of limited practical application in traditional programs [4]. By guiding students through a multi-day (currently designed to be four-day long) hands-on training workshop, the HOPE Kits enable participants to apply their theoretical thinking, problem-solving skills, and the ability to troubleshoot PIC devices, preparing students for the challenges they may encounter in a professional setting. Furthermore, the HOPE Kits provide a platform for students to engage in data analysis interpretation, a vital aspect of integrated photonics research and development. Through the provided written script and accompanying questions, participants are encouraged to analyze the experimental data collected during the workshop. This process enhances their data analysis skills and allows them to draw meaningful conclusions from the results.

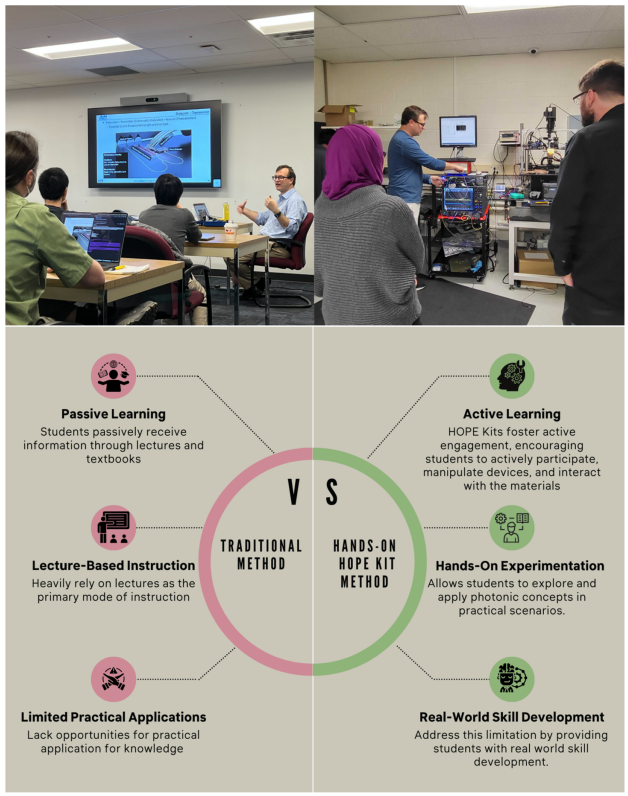

Fig. 15. Illustrating the comparison between the traditional teaching method and the HOPE Kit approach.

We are working to engage additional institutions, creating a network for hands-on integrated photonics training. As an example, the Commonwealth of Massachusetts has created five Laboratories for Education and Application Prototypes (LEAPs) strategically located across the state [15]. Laboratory projects, bootcamps, summer internships, and workshops using HOPE Kits will positively impact the education of students at research institutions; students and faculty from high schools, community colleges, and four-year colleges; as well as company employees. Such a LEAP education model for expanding outreach can be replicated across the country to ramp up training of the workforce in electronic–photonic integration, a much needed skill set for the CHIPS ecosystem.

In the future we plan to expand the capabilities and applications of the HOPE Kits. Specifically, integrated lasers are being developed in order to realize complete data communication links. In addition, we are investigating HOPE Kits for emerging applications of integrated photonics, such as sensing, LiDAR, artificial intelligence, and quantum.

In conclusion, the HOPE Kits have significant implications for the integrated photonics training ecosystem. By promoting active learning, providing practical application opportunities, and nurturing a comprehensive skill set, the HOPE Kits bridge the gap between theoretical knowledge and industry demands. Graduates trained with the HOPE Kits are better equipped to meet the increasing workforce demands in the photonics industry, contributing to the growth and advancement of this

critical sector. Adopting the HOPE Kits in photonics training programs has the potential to revolutionize the way students learn and prepare for successful careers in the dynamic field of integrated photonics.

Funding. Air Force Research Laboratory (FA8650-21-2-1000).

Acknowledgment. We acknowledge AIM Photonics for its support. This material is based on research sponsored by the Air Force Research Laboratory. The U.S. Government is authorized to reproduce and distribute reprints for Governmental purposes, notwithstanding any copyright notation thereon. The views and conclusions contained herein are those of the authors and should not be interpreted as necessarily representing the official policies or endorsements, either expressed or implied, of the United States Air Force, the Air Force Research Laboratory, or the U.S. Government.

Disclosures. The authors declare no conflicts of interest.

Data availability. Data underlying the results presented in this paper are not publicly available at this time but may be obtained from the authors upon reasonable request.

REFERENCES

1. E. Moore, F. R. Field, S. Saini, R. Roth, L. C. Kimerling, G. Westerman, and R. Kirchain, "Adaptable middle-skilled labor: a neglected roadblock to photonics industry growth," Appl. Opt. **62**, H9–H16 (2023).
2. R. Breault, "Workforce development for harnessing light," Proc. SPIE **3831**, 76–79 (2000).
3. R. Kirchain, E. Moore, F. Field, S. Saini, and G. Westerman, "Preparing the advanced manufacturing workforce," in *AIM Photonics and MIT Office of Open Learning* (2021).
4. J. Arango, S. Bechtold, P. Bedoya-Ríos, and S. Serna, "Nonlinear photonics in undergraduate curriculum: hands-on training to meet the demands of a qualified workforce," Proc. SPIE **12213**, 114–143 (2022).
5. L. Chrostowski and M. Hochberg, *Silicon Photonics Design: From Devices to Systems* (Cambridge University, 2015).
6. K. S. M. Glick and L. Liao, *Integrated Photonics for Data Communication Applications* (Elsevier, 2023).
7. J. Wang, M. M. Sanchez, Y. Yin, R. Herzer, L. Ma, and O. G. Schmidt, "Silicon-based integrated label-free optofluidic biosensors: latest advances and roadmap," Adv. Mater. Technol. **5**, 1901138 (2020).
8. E. Pelucchi, G. Fagas, I. Aharonovich, D. Englund, E. Figueroa, Q. Gong, H. Hannes, J. Liu, C.-Y. Lu, N. Matsuda, and J. W. Pan, "The potential and global outlook of integrated photonics for quantum technologies," Nat. Rev. Phys. **4**, 194–208 (2022).
9. A. N. Tait, T. F. De Lima, E. Zhou, A. X. Wu, M. A. Nahmias, B. J. Shastri, and P. R. Prucnal, "Neuromorphic photonic networks using silicon photonic weight banks," Sci. Rep. **7**, 7430 (2017).
10. C. V. Poulton, A. Yaacobi, D. B. Cole, M. J. Byrd, M. Raval, D. Vermeulen, and M. R. Watts, "Coherent solid-state lidar with silicon photonic optical phased arrays," Opt. Lett. **42**, 4091–4094 (2017).
11. L. Labios and A. E. Amili, "Engineers developing education kit to teach students practical skills in integrated photonics," UC San Diego Today (2019).
12. S. Serna, N. Hidalgo, J. Tjan, K. McComber, L. Kimerling, E. Verlage, J. Diop, J. Hu, S. Saini, A. Agarwal, and G. Gagnon, "A modular laboratory curriculum for teaching integrated photonics to students with diverse backgrounds," in *Education and Training in Optics and Photonics* (Optica, 2019), p. 11143_142.
13. S. Saini, S. Preble, M. Popović, J. Cardenas, A. Kost, E. Verlage, G. Howland, and L. C. Kimerling, "Integrated photonics and application-specific design on a massive open online course platform," in *Education and Training in Optics and Photonics* (Optica, 2019), p. 11143_151.
14. E. Verlage, S. Saini, A. Agarwal, S. Serna, R. Kosciolek, T. Morrisey, and L. C. Kimerling, "Web-based interactive simulations and virtual lab for photonics education," in *Education and Training in Optics and Photonics* (Optica, 2019), p. 11143_136.
15. D. M. Weninger, S. Serna, S. Saini, L. Ranno, E. Verlage, S. Bechtold, P. Bedoya-Rios, J. Hu, L. Kimerling, and A. M. Agarwal, "The Massachusetts LEAP network: building a template for a hands-on advanced manufacturing hub in integrated photonics," Proc. SPIE **12723**, 380–387 (2023).
16. N. M. Fahrenkopf, C. McDonough, G. L. Leake, Z. Su, E. Timurdogan, and D. D. Coolbaugh, "The aim photonics MPW: a highly accessible cutting edge technology for rapid prototyping of photonic integrated circuits," IEEE J. Sel. Top. Quantum Electron. **25**, 1–6 (2019).
17. L. Liao, D. Samara-Rubio, M. Morse, A. Liu, D. Hodge, D. Rubin, U. D. Keil, and T. Franck, "High speed silicon Mach-Zehnder modulator," Opt. Express **13**, 3129–3135 (2005).
18. M. Streshinsky, R. Ding, Y. Liu, A. Novack, Y. Yang, Y. Ma, X. Tu, E. K. S. Chee, A. E.-J. Lim, P. G.-Q. Lo, and T. Baehr-Jones, "Low power 50 Gb/s silicon traveling wave Mach-Zehnder modulator near 1300 nm," Opt. Express **21**, 30350–30357 (2013).
19. L. Chen and M. Lipson, "Ultra-low capacitance and high speed germanium photodetectors on silicon," Opt. Express **17**, 7901–7906 (2009).
20. G. Li, Y. Luo, X. Zheng, G. Masini, A. Mekis, S. Sahni, H. Thacker, J. Yao, I. Shubin, K. Raj, and J. E. Cunningham, "Improving CMOS-compatible germanium photodetectors," Opt. Express **20**, 26345–26350 (2012).
21. S. Manipatruni, L. Chen, and M. Lipson, "Ultra high bandwidth WDM using silicon microring modulators," Opt. Express **18**, 16858–16867 (2010).
22. Q. Xu, B. Schmidt, S. Pradhan, and M. Lipson, "Micrometre-scale silicon electro-optic modulator," Nature **435**, 325–327 (2005).
23. M. Gad, J. Ackert, D. Yevick, L. Chrostowski, and P. Jessop, "Ring resonator wavelength division multiplexing interleaver," J. Lightwave Technol. **29**, 2102–2109 (2011).
24. R. Boeck, "Silicon ring resonator add-drop multiplexers," Ph.D. thesis (University of British Columbia, 2011).
25. D. Dai and J. E. Bowers, "Silicon-based on-chip multiplexing technologies and devices for peta-bit optical interconnects," Nanophotonics **3**, 283–311 (2014).
26. L. Han, B. P.-P. Kuo, A. Pejkic, N. Alic, and S. Radic, "50GHz silicon cascaded Mach-Zehnder wavelength filter and automatic phase error correction," in *Optical Fiber Communications Conference and Exhibition (OFC)* (IEEE, 2019), pp. 1–3.
27. M. Hammood, A. Mistry, H. Yun, M. Ma, L. Chrostowski, and N. A. Jaeger, "Four-channel, silicon photonic, wavelength multiplexer-demultiplexer with high channel isolations," in *Optical Fiber Communication Conference* (Optica, 2020), paper M3F-5.
28. C. Kaalund, "Critically coupled ring resonators for add-drop filtering," Opt. Commun. **237**, 357–362 (2004).
29. J.-M. Lee, "Athermal silicon photonics," in *Silicon Photonics III*, L. Pavesi and D. J. Lockwood, eds. (SpringerNature, 2016), Chap. **3**, pp. 83–98.
30. P. Dong, R. Shafiiha, S. Liao, H. Liang, N.-N. Feng, D. Feng, G. Li, X. Zheng, A. V. Krishnamoorthy, and M. Asghari, "Wavelength-tunable silicon microring modulator," Opt. Express **18**, 10941–10946 (2010).
31. T. Baba, S. Akiyama, M. Imai, N. Hirayama, H. Takahashi, Y. Noguchi, T. Horikawa, and T. Usuki, "Efficient 50-Gb/s silicon microring modulator based on forward-biased pin diodes," in *10th International Conference on Group IV Photonics* (2013).
32. R. Soref and B. Bennett, "Electrooptical effects in silicon," IEEE J. Quantum Electron. **23**, 123–129 (1987).
33. M. Nedeljkovic, R. A. Soref, and G. Z. Mashanovich, "Free-carrier electrorefraction and electroabsorption modulation predictions for silicon over the 1–14-μm infrared wavelength range," IEEE Photon. J. **3**, 1171–1180 (2011).
34. AIM Photonics, "Aim photonics boot camps and workshops," https://www.aimphotonics.com/boot-camp.